The magnetic composition–temperature phase diagram of the kagome mixed system $(Co_xNi_{1-x})_3V_2O_8$



2008 J. Phys.: Condens. Matter 20 095219

(http://iopscience.iop.org/0953-8984/20/9/095219)

J. Phys.: Condens. Matter **20** (2008) 095219 (5pp) doi:10.1088/0953-8984/20/9/095219

# The magnetic composition–temperature phase diagram of the kagome mixed system $(Co_xNi_{1-x})_3V_2O_8$

**N Qureshi[1,2], H Fuess[1], H Ehrenberg[3], T C Hansen[2], C Ritter[2], P Adelmann[4], C Meingast[4], Th Wolf[4], Q Zhang[4] and W Knafo[4,5]**

[1] Institute for Materials Science, University of Technology, D-64287 Darmstadt, Germany
[2] Institut Max von Laue-Paul Langevin, 38042 Grenoble Cedex 9, France
[3] Institute for Complex Materials, IFW Dresden, D-01069 Dresden, Germany
[4] Research Center Karlsruhe, Institute of Solid State Physics, D-76021 Karlsruhe, Germany
[5] Physics Institute, Karlsruhe University, D-76128 Karlsruhe, Germany

E-mail: navidq@st.tu-darmstadt.de

Received 26 October 2007, in final form 25 January 2008
Published 14 February 2008
Online at stacks.iop.org/JPhysCM/20/095219

**Abstract**

The magnetic composition–temperature ($x$–$T$) phase diagram of the mixed kagome system $(Co_xNi_{1-x})_3V_2O_8$ (CNVO) deduced from neutron powder diffraction and single-crystal heat capacity experiments is presented. CNVO changes its magnetic structure twice below 5.5 K as a function of the compositional parameter $x$. A sample with $x = 0.98$ has been found to be of a critical composition where both ferromagnetic and antiferromagnetic reflections of the $Co_3V_2O_8$ (CVO) type magnetic structure have been observed in the diffraction pattern. Below this composition the ferromagnetic phase is completely suppressed and antiferromagnetic short-range order is present, which is modulated by a propagation vector $\mathbf{k}_1 = (0, \delta, 0)$ with $\delta$ being temperature and composition dependent. Below 4.2 K $\delta$ has a constant value of 0.4 for $0.76 < x < 0.92$. In the region $0.71 < x < 0.76$ a change of the magnetic structure into the long-range ordered $Ni_3V_2O_8$ (NVO) type with $\mathbf{k}_2 = (\delta, 0, 0)$, where $\delta$ is only dependent on $x$, takes place. Finally, for $x < 0.035$ the positions of the magnetic reflections become temperature dependent again.

(Some figures in this article are in colour only in the electronic version)

## 1. Introduction

The mixed system $(Co_xNi_{1-x})_3V_2O_8$ (CNVO) of isostructural parent compounds $Ni_3V_2O_8$ (NVO) and $Co_3V_2O_8$ (CVO) belongs to the transition metal (M) orthooxovanadates, whose crystal structures are characterized by a kagome staircase geometry. Hereby, spin-1 Ni and spin-$\frac{3}{2}$ Co statistically occupy the crystallographic sites (4a) and (8e) of space group *Cmca* [1, 2] with the Co ions having a slight affinity [3, 4] for the (4a) sites. This results in buckled planes of corner-sharing isosceles triangles, whose corners are occupied by magnetic ions, representing an anisotropic variation of the ideal kagome net. Within these layers the magnetic interactions are mainly effectuated via nearly 90° M–O–M superexchange pathways between the edge-sharing $MO_6$ octahedra. Neighboring staircases along the *b*-axis are separated by nonmagnetic $VO_4$ tetrahedra and coupled by supersuperexchange. Due to the lowered degree of frustration, NVO and CVO exhibit sequences of four [5, 6] and five [7] magnetic phase transitions, respectively. In contrast to this, the investigation of CNVO powder ($x = 0.27, 0.52, 0.76$) [4] and single-crystal samples ($x = 0.53$) [8] with neutron diffraction, magnetization and heat capacity experiments revealed only one magnetic phase transition into an antiferromagnetic ground state. Due to the fact that CVO exhibits intermediate antiferromagnetic phases ($AF_1$) modulated by $\mathbf{k}_1 = (0, \delta, 0)$ and a ferromagnetic ground state (FM) [7, 9] compared to the antiferromagnetic ones of CNVO ($AF_2$) with $\mathbf{k}_2 = (\delta, 0, 0)$, at least one compositional magnetic phase boundary has to occur. In this work we present the magnetic ($x$–$T$) phase diagram derived from

 

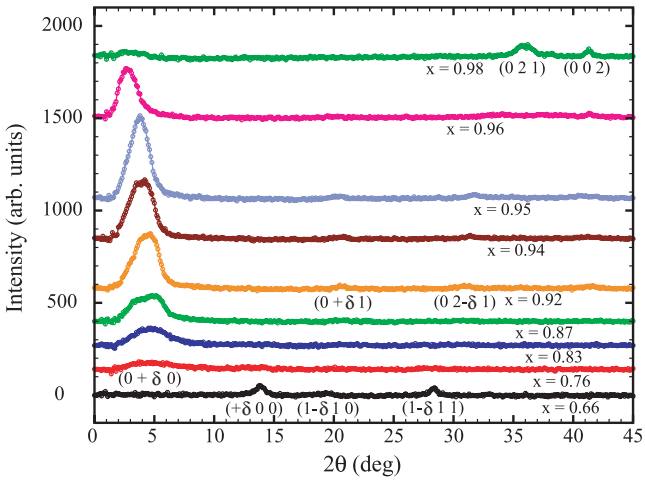


**Figure 1.** Magnetic scattering of $(Co_xNi_{1-x})_3V_2O_8$ powder samples with different values of $x$ at 1.5 K and zero field obtained by measurements using D1A. The patterns are shifted vertically for clarity.

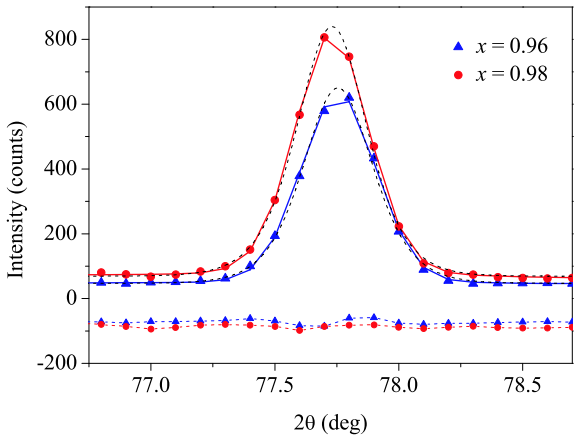


**Figure 2.** Nuclear (042) reflection for $x = 0.96$ (triangles) and $x = 0.98$ (circles) at 20 K. The straight lines connect the calculated points (not depicted) obtained by a fit with pseudo-Voigt functions (dashed lines with respective symbols represent the difference curves). The dashed lines without symbols are the result of the asymmetric double-sigmoid fit.

neutron powder diffraction and single-crystal heat capacity measurements, which shows two clear compositional magnetic phase boundaries below $T = 5.5$ K.

## 2. Experimental details

$(Co_xNi_{1-x})_3V_2O_8$ powder samples were synthesized using a method similar to the one presented in [10], where the stoichiometrically mixed starting oxides NiO, CoO and $V_2O_5$ were sintered at 1050 °C first for one and then for four days with intermediate grindings. The samples were investigated using a high-resolution (D1A) and a high-intensity neutron powder diffractometer (D20) at the Institut Laue-Langevin using wavelengths of 2.99 Å supplied by the (113) reflection of a Ge monochromator and 2.41 Å from the (002) reflection of a pyrolytic graphite HOPG monochromator. Each sample was measured in the paramagnetic regime at 20 K in order to extract the nuclear structure and especially the compositional parameter $x$. The investigation of the magnetic properties was performed at 1.5 K. Measurements on all powder samples were made using D1A except for the samples with $x = 0$, 0.35 and 0.71, for which D20 was used, and those with $x = 0.87$, 0.92 and 0.98, for which both instruments were used. Single crystals with concentrations $x = 0, 0.5, 0.65, 0.86$ and 1.0 were grown from self-flux. The compositions of the mixed crystals were estimated using lattice parameters determined using x-ray powder diffraction and Vegard's law. The specific heat was measured using a PPMS from Quantum Design. The data around the phase transitions were obtained by analyzing individual relaxation curves after a large (2–3 K) temperature pulse via a method similar to the one presented in [11].

## 3. Results

Neutron diffraction experiments on the respective powder samples within the paramagnetic phases (PM) at 20 K revealed the correct phase formation of the orthorhombic structures (space group *Cmca*). The refinement process included the cell parameters, the atomic positions of M and O, an overall isotropic temperature factor and the Co:Ni ratio. The atomic position of V has been fixed in all refinements because of its low coherent neutron scattering cross section. The resolution parameters $u$, $v$ and $w$ as well as the ratios source width/detector distance and detector width/detector distance, which indicate the asymmetry of the reflection profiles, have been set according to the instrument resolution function. The recorded diffraction patterns of the paramagnetic phases (20 K) were subtracted from the respective magnetically ordered ones (1.5 K) in order to emphasize the magnetic scattering, which is depicted in figure 1. It was found that substituting 2% of Co with Ni results in a critical composition where both ferromagnetic ($2\theta = 36°$ and 41°) and antiferromagnetic ($2\theta \approx 3°$) reflections of the CVO magnetic structure type can be observed. However, the antiferromagnetic ($0+\delta$ 0) reflection is very low in intensity, but significant if compared to the diffraction pattern of the $x = 0.66$ sample. In order to be precise on the critical values especially with respect to the uniformity of the powder samples investigated the reflection profile has been examined in detail: the ratio between Co and Ni on the magnetic sites determines the cell constants according to Vegard's law; therefore the peak positions are dependent on the composition. Assuming a distribution of compositions within one powder sample, one would expect enlarged reflection profiles due to the different contributions. In the case of a random distribution an asymmetry of the reflection profile may be observed. To clarify this point the profile of the nuclear (042) reflection, which is strong, isolated from others and close to the minimum of the resolution curve of the instrument, has been focused on (figure 2). The raw data points (triangles stand for $x = 0.96$, circles represent $x = 0.98$) have been fitted with pseudo-Voigt functions, whose FWHM are defined only by the fixed instrument resolution and asymmetry parameters (where the latter do not affect the peak profile at such high angles anyway). The calculated points

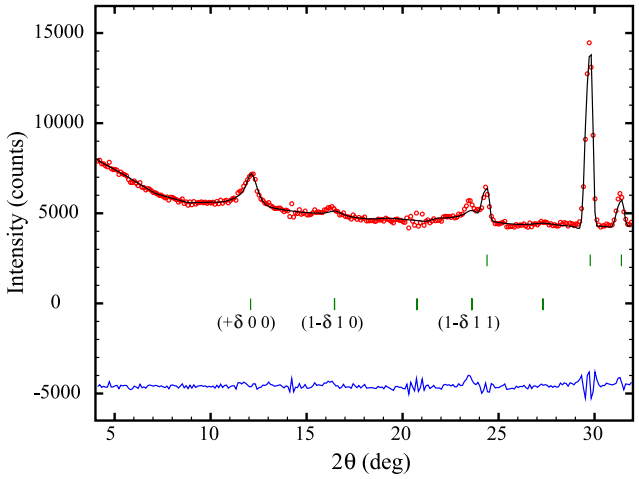


**Figure 3.** Observed pattern (circles), calculated pattern (upper (black) line) and difference plot (lower (blue) line) of $(Co_{0.71}Ni_{0.29})_3V_2O_8$ at 1.5 K and zero field revealing the NVO modulation type with $\mathbf{k}_2 = (0.522(7), 0, 0)$.

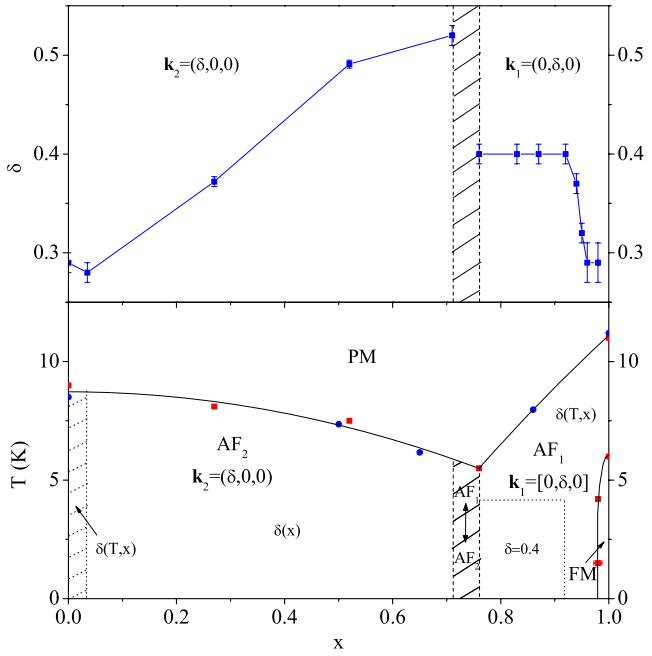


**Figure 4.** Upper panel: incommensurabilities $\delta$ as a function of the compositional parameter $x$ at $T = 1.5$ K. Lower panel: magnetic $(x, T)$ phase diagram of $(Co_xNi_{1-x})_3V_2O_8$ obtained from neutron powder diffraction ((red) squares) and single-crystal heat capacity ((blue) dots) experiments.

(not shown, but connected with straight lines) show excellent agreement with the observed data. From the difference plots (dashed lines with respective symbols) a minimal asymmetry might be observed. Therefore, the raw data have been fitted with an asymmetric double-sigmoidal function, which is characterized by $w_1$ giving the main FWHM of the curve and additional parameters $w_2$ and $w_3$ describing the asymmetry on either side of the peak. The refined values are $w_2 = 0.092(8)$ and $w_3 = 0.094(7)$ for the $x = 0.96$ sample and $w_2 = 0.096(2)$ and $w_3 = 0.092(6)$ for $x = 0.98$ showing that no significant asymmetry exists. The fact that the reflection profile is neither enlarged nor asymmetric leads to the conclusion that the powder samples investigated are uniform within the limits of precision of the diffractometer. From the standard deviations of the refined occupation parameters a standard deviation of the composition of less than 0.01 can be deduced for each sample.

Below $x = 0.98$ the ferromagnetic phase is completely suppressed for $T \geqslant 1.5$ K with the antiferromagnetic structure being modulated by $\mathbf{k}_1$ with $\delta = f(T, x)$. But it is only for $x$ between 0.92 and 0.95 that additional magnetic reflections $[(0+\delta\ 1)$ and $(0\ 2-\delta\ 1)]$ can be observed and indexed. Below $x = 0.92$ these reflections disappear; furthermore, the fundamental reflection becomes weaker and much broader than the predicted peak width, but even the better defined magnetic reflections are considerably larger than the instrumental resolution, giving rise to the assumption that only antiferromagnetic short-range order is present. This case is the same for $x > 0.95$ with the difference that no information about the peak width can be deduced, because the $(000)^+$ reflection profile is influenced by the high background due to its very small diffraction angle. In contradiction to [4] it can be seen, due to there being more samples on the Co rich side, that for $x = 0.76$, which is exactly the same powder sample, the $(000)^+$ reflection of the CVO type can still be observed in a broad and weak form (figure 1). Hence, as for $x = 0.71$ the magnetic reflections can be indexed by a propagation vector $\mathbf{k}_2 = [0.522(7), 0, 0]$ (figure 3), the critical composition, where the magnetic structure switches from the CVO to the NVO type, has to be in the region $0.71 < x < 0.76$. It can be seen from the refinement that the widths of the magnetic reflections are consistent with the instrument resolution, revealing long-range ordered antiferromagnetism for $x < 0.71$. By indexing the magnetic reflections of the respective neutron diffraction patterns the composition dependence of the incommensurabilities $\delta$ could be deduced (upper panel of figure 4), but it should be mentioned that a precise determination of the propagation vector of the samples with $x > 0.95$ turned out to be difficult owing to background problems as mentioned above.

As previously observed for $x = 0.27$ and 0.52 [4], the positions of the magnetic reflections only change with composition and not with temperature, whereas the NVO magnetic structure exhibits a temperature dependent propagation vector [5]. From measurements using D20 it was revealed that a substitution of 3.5% Ni with Co suppresses the aforementioned temperature dependence, which is shown in figure 5. Similarly, it was observed, from thermodiffractograms with temperature steps of 0.1 K, that the previously reported temperature dependence of the propagation vector of the CVO magnetic structure [7] becomes weak on reaching a composition of $x = 0.87$ (figure 6(a)). Only a slight shift of the fundamental $(000)^+$ reflection can be observed above approximately 4 K (exact determination of results was difficult due to the rather weak reflection compared to the background). The temperature dependent shift of the magnetic reflections can be clearly seen in figures 6(b) and (c). For the $x = 0.92$ sample, in figure 6(b) the magnetic reflections appear at 8.6(1) K and can be indexed by a propagation vector

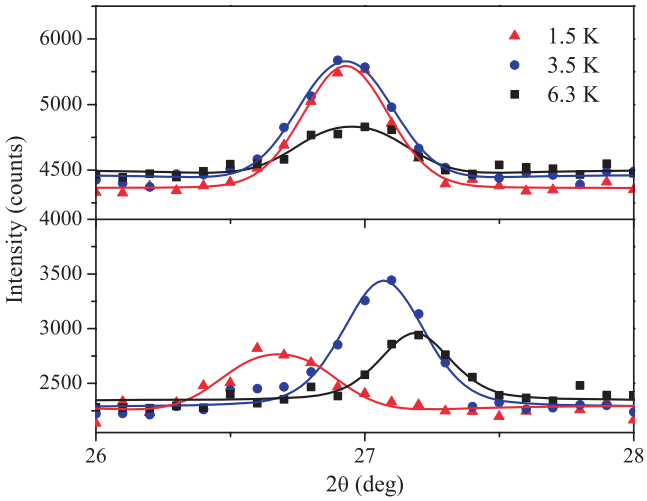


**Figure 5.** Magnetic $(1-\delta\,11)$ reflection for $x = 0$ (lower panel) and $x = 0.035$ (upper panel). The data points have been fitted with pseudo-Voigt functions. The temperature dependent shift of the magnetic reflection can clearly be seen for $x = 0$, where it does not exist for $x = 0.035$.

$\mathbf{k}_1 = (0, 0.5, 0)$. Between 8.6(1) K and 4.2(1) K the positions of the magnetic reflections vary with temperature until they lock in at 4.2(1) K with $\mathbf{k}_1 = (0, 0.4, 0)$. In the case of $x = 0.98$ depicted in figure 6(c) one can observe a temperature dependent shift of the magnetic reflections throughout the antiferromagnetic phase without any lock-ins. The magnetic phase transition into the ferromagnetic phase takes place at 4.2(1) K. Heat capacity measurements were performed on the pure Ni and Co compounds and on three intermediate ones ($x = 0.5, 0.65$ and 0.86). Figure 7 shows the specific heat in a $C_p/T$ versus $T$ plot. The data for NVO and CVO exhibit the same sequence of transitions and are qualitatively similar to the data reported previously [5, 7, 12]. $C_p/T$ is, however, up to a factor of 10 larger at the first-order incommensurate to commensurate magnetic transitions at about 3.8 K (NVO) and 6 K (CVO) than the data in [5, 7, 12], which were also all acquired using a PPMS. This large difference is due to the inadequacy of the standard PPMS software in dealing with sharp first-order phase transitions. For CVO especially, a large part of the magnetic entropy is gained at this first-order transition, which is missed by using the standard PPMS specific heat data acquisition. For the mixed crystals ($x = 0.5, 0.65$ and 0.86) only a single sharp feature indicating a phase transition is observed down to the lowest measured temperature of 2 K in agreement with [4]. These transition temperatures are plotted in the lower panel of figure 4 together with those determined from the magnetic neutron scattering data. Good agreement is found between the two sets of transition temperatures, confirming the Vegard's law approximation of the single-crystal Co contents. A more detailed analysis of the specific heat data together with high-resolution thermal expansion data will be presented in a separate publication [13].

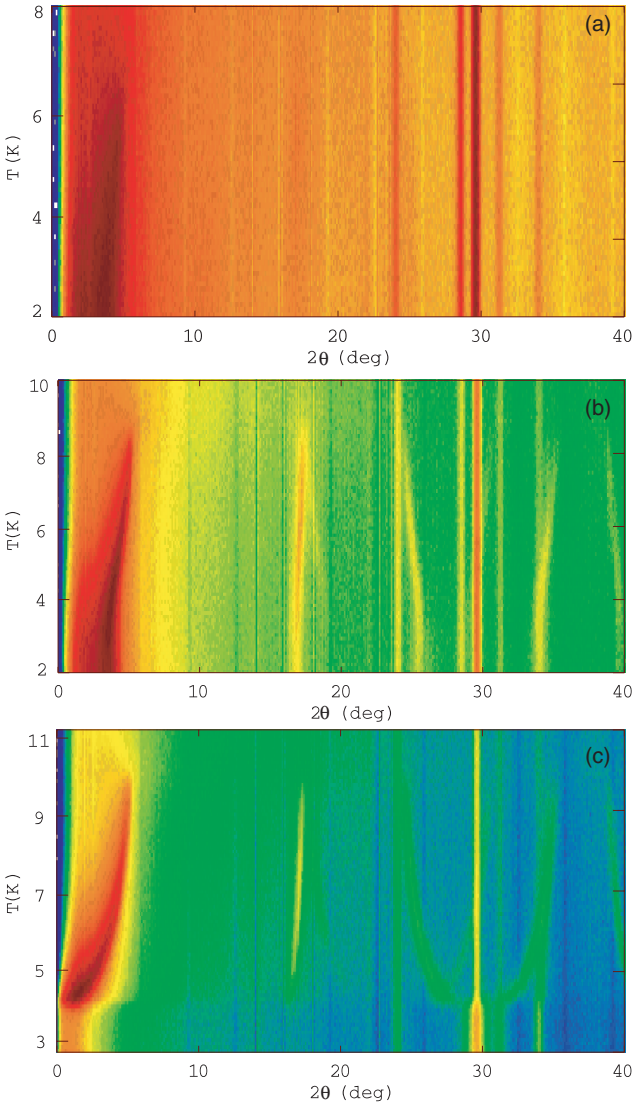


**Figure 6.** Thermodiffractograms of powder samples with $x = 0.87$ (a), 0.92 (b) and 0.98 (c) revealing the temperature dependent shift of the magnetic reflections for (b) and (c), which can hardly be observed for (a).

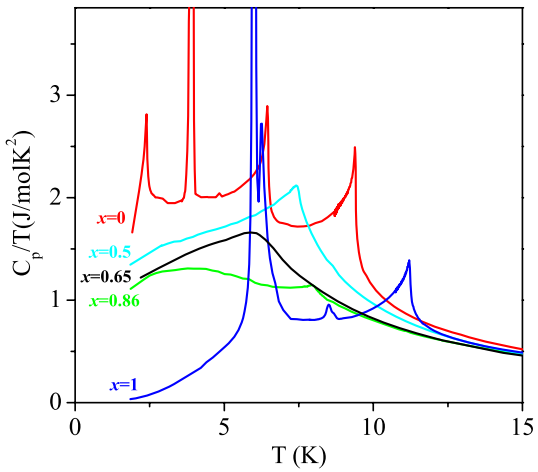


**Figure 7.** Heat capacity curves as a function of temperature revealing a single phase transition for the mixed crystals.

## 4. Discussion

The magnetic phase transitions of the $(Co_xNi_{1-x})_3V_2O_8$ system have been examined as a function of temperature and composition by means of neutron powder diffraction and single-crystal heat capacity experiments. The transition points obtained by the two methods match up well and are plotted together in the magnetic $(x, T)$ phase diagram (lower panel of figure 4), which is shown here in detail for the first time. A preliminary phase diagram was reported by Zhang *et al* [14]. One can observe a decrease of $T_N$ with increasing amount of $M^{2+}$ substitution starting from either end of the phase diagram, until the lowest observed Néel temperature of 5.5 K is reached with $x = 0.76$. This composition still exhibits a CVO type modulation, while $x = 0.71$ is modulated by $\mathbf{k}_2$, which indicates a change of the magnetic structure for $0.71 < x < 0.76$ into the antiferromagnetic long-range ordered NVO type. Furthermore, it has been deduced that small degrees of magnetic ion substitution disturb the magnetic structures of the parent compounds. Substituting 2% of Co with Ni leads to a suppression of the ferromagnetic CVO ground state in favor of the antiferromagnetic short-range ordered CVO phase with $\mathbf{k}_1 = [0, \delta(T, x), 0]$. On the other hand, 3.5% Co on the magnetic sites of NVO removes the temperature dependence of its propagation vector $\mathbf{k}_2$. A further interesting result is the existence of a phase within $AF_1$ with $\delta$ having a constant value of 0.4, which is the case for $T < 4.2$ K and $0.76 < x < 0.92$. These findings allow us to draw a preliminary phase boundary inside the $AF_1$ phase (dotted lines in figure 4). The richness of different magnetic structures and modulation types underlines the sensitive energy balance of exchange interactions along various coupling pathways in the kagome mixed system $(Co_xNi_{1-x})_3V_2O_8$, which is worth finding an explanation for on a theoretical level; this should be the aim of future investigations.

## Acknowledgments

This research was supported by the *Deutsche Forschungsgemeinschaft* within the priority program 1178. Part of this work was supported by the *Helmholtz Association of German Research Centers* through the Virtual Institute of Research on Quantum Phase Transitions and Project VH-NG-016.

## References

[1] Fuess H, Bertaut E F, Pauthenet R and Durif A 1970 *Acta Crystallogr.* B **26** 2036
[2] Sauerbrei E E, Faggiani R and Calvo C 1973 *Acta Crystallogr.* B **29** 2304
[3] Wang P L, Werner P E and Nord A G 1992 *Z. Kristallogr.* **198** 271
[4] Qureshi N, Fuess H, Ehrenberg H, Hansen T C, Ritter C, Prokes K, Podlesnyak A and Schwabe D 2006 *Phys. Rev.* B **74** 212407
[5] Lawes G *et al* 2004 *Phys. Rev. Lett.* **93** 247201
[6] Kenzelmann M *et al* 2006 *Phys. Rev.* B **74** 014429
[7] Chen Y *et al* 2006 *Phys. Rev.* B **74** 014430
[8] Qureshi N, Fuess H, Ehrenberg H, Ouladdiaf B, Hansen T C, Wolf T, Meingast C, Zhang Q, Knafo W and von Löhneysen H 2008 *J. Phys.: Condens. Matter* submitted
[9] Qureshi N, Fuess H, Ehrenberg H, Hansen T C and Schwabe D 2007 *Solid State Commun.* **142** 169
[10] Balakrishnan G, Petrenko O A, Lees M R and Paul D M K 2004 *J. Phys.: Condens. Matter* **16** L347
[11] Lashley J C *et al* 2003 *Cryogenics* **43** 369
[12] Szymczak R, Baran M, Diduszko R, Fink-Finowicki J, Gutowska M, Szewczyk A and Szymczak H 2006 *Phys. Rev.* B **73** 094425
[13] Zhang Q 2008 in preparation
[14] Zhang Q, Knafo W, Grube K, von Löhneysen H, Meingast C and Wolf T 2007 *Physica* B at press doi:10.1016/j.physb.2007.10.363